OSCILLATOR STRENGTHS FOR THE N_2 SECOND POSITIVE AND N_2^+ FIRST NEGATIVE SYSTEMS FROM OBSERVATIONS OF [redacted] SHOCK LAYERS ABOUT HYPERSONIC PROJECTILES

By Victor H. Reis*

National Aeronautics and Space Administration
Ames Research Center
Moffett Field, Calif.

ABSTRACT

The electronic oscillator strengths, f, for the N_2 second positive and N_2^+ first negative systems were determined by measuring the radiation from the shock layer about a hypervelocity projectile with a time-of-flight scanning spectrometer. The measured values at the $\Delta v = 0$ bands were $f = 0.057 \pm 0.01$ for $N_2(2+)$ and $f = 0.053 \pm 0.01$ for $N_2(1-)$. The variation of f with wavelength for both systems was found to be similar to that previously reported by Nicholls.

Author

INTRODUCTION

Measurements of radiant emission from shock-heated gases have been demonstrated[1] to yield values of oscillator strengths in reasonable agreement with values obtained by electron beam excitation.[2] In previous studies of radiation from shock-heated gases, the gas was energized by shock waves generated in shock tubes. The present investigation utilizes the gas in the shock layer behind the bow shock waves of small blunt models flying at hypersonic velocities into nitrogen as the source of radiation. Continuously recorded spectra are obtained photoelectrically by means of a time-of-flight scanning spectrometer

*Research Scientist

and reduced to obtain oscillator strengths (f-numbers) for the N_2 second positive $C^3\pi_u - B^3\pi_g$ and N_2^+ first negative $B^2\Sigma_u^+ - X^2\Sigma_g^+$ systems. Nitrogen was chosen as the test gas because of its relatively well-known thermodynamic and spectroscopic properties as well as its importance in atmospheric physics and as a contributor to the radiative heating of vehicles entering planetary atmospheres at hypersonic speeds.

EXPERIMENTAL TECHNIQUE

The models were lauched from the two-stage shock-heated 0.28-caliber light-gas gun of the pilot hypervelocity free-flight facility at the NASA, Ames Research Center.[3] The experimental setup is sketched in Fig. 1. The models were made of aluminum or a polyformaldehyde plastic. Because of the short flight distance the aerodynamic heating of the models was such that the aluminum surface remained relatively cool, whereas the surface of the plastic model ablated. However, as there was no measurable difference in the data obtained with the two different model materials, the plastic models were used more extensively since they were easier to launch successfully. In addition to the time-of-flight scanning spectrometer (described below) the instrumentation included shadowgraph stations and electronic counters to obtain the velocity and attitude of the model and an Abtronics 2HS image-converter camera. Relatively broad-band radiometers, each consisting of a multiplier phototube fitted with entrance and collimating slits and a band-pass filter, were used as a check on the over-all level of radiation seen by the scanning spectrometer. The radiometers also

allowed crude determination of the spatial distribution of radiation in the flow field. The use of such broad-band devices is described by Craig and Davy.(4)

Samples of the nitrogen were taken immediately prior to shooting and analyzed with a C.E.C. 21620 mass spectrometer. Typically, the contaminants, oxygen, argon, and water vapor, were held to trace amounts and never exceeded 0.2 percent.

TIME-OF-FLIGHT SCANNING SPECTROMETER

Spectra were obtained photoelectrically by means of a time-of-flight scanning spectrometer.* This device is shown schematically in Fig. 2. As the model flies by in the focal plane of the collecting mirror, the luminous gas cap acts as a moving entrance slit, sweeping out the spectrum of the shock-heated gas on the exit slit. (That the gas cap is the only source of radiation in the flow field and is indeed slitlike in form is shown in a typical image-converter photograph of a plastic model and in a typical oscillogram of a broad-band radiometer (Fig. 3).) The energy passing through the exit slit of scanning spectrometer is divided; 95 percent passes through a splitter plate and on to the cathode of an RCA 1P28 multiplier phototube. The output of this multiplier phototube is recorded on an oscilloscope and yields a continuously recorded spectrum over a wavelength range dictated mainly by the geometry of the system. For the tests reported in this work, the wavelength range was as a rule from 0.290 to 0.430 μ. Figure 4(a) shows a typical oscillogram. The remaining 5 percent of

*The concept for such a device appears to have originated with E. L. Woodcock and B. Jones.(5)

the energy passes through a narrow-band interference filter (100 Å half width) and onto a Dumont 6935 multiplier phototube. The output of this side band is displayed on an oscilloscope which has been triggered so as to start sweeping simultaneously with the oscilloscope which records the spectra. The side-band oscillogram thus allows a specific wavelength to be transposed to the oscillogram displaying the spectra. Such wavelength transposition was found to be repeatable from shot to shot to ±10Å.

The time-of-flight scanning spectrometer was constructed by modifying a Farrand uv-vis f/3.5 grating monochromator. A large opening was cut in the monochromator housing in the region of the entrance slit and the collecting mirror was replaced by a spherical mirror which focused at the center of the test chamber. Further, the new collecting mirror was masked down to a rectangular slot to improve depth of field and to insure uniform illumination of the grating. The rise time of the complete system was 25 nanoseconds and was dictated by the oscilloscope.

CALIBRATION

Wavelength calibration of the spectrometer was accomplished with a mercury lamp and appropriate color filters, both on a bench and in the test section. The complete optical train was calibrated with a tungsten ribbon filament lamp which had been previously compared with a primary standard supplied by the National Bureau of Standards.[6] The calibration curve for the complete optical train is shown in Fig. 4(b). The calibration was checked before and after each series of experiments.

EXPERIMENTAL RESULTS

Time-of-flight scanning spectrometer oscillograms were obtained for a range of model velocities of from 4.6 to 5.8 km/sec and ambient densities of 0.07 to 0.2 amagat. The calculated equilibrium temperatures throughout the shock layer ranged from 6000° to 7700° K. A typical oscillogram is shown in Fig. 4(a), and Fig. 4(c) shows this oscillogram reduced to absolute levels through the calibration curve (Fig. 4(b)). The wavelength scale on the oscillogram is nonlinear because the model flies on a tangent to the focal plane of the collecting mirror and because of slight nonlinearities in the oscilloscope horizontal sweep. Results such as shown in Fig. 4(c) were found to be quite reproducible. The wavelengths of the peaks were repeated to within ±10Å over the entire range of experiments or at about the limit of accuracy for reading the oscillogram. In addition two shots at almost identical flight conditions gave results which agreed within 10 percent in absolute levels of radiation.

The peak values of radiant intensity were never greater than 1 percent of an equivalent black body, calculated at an average shock-layer temperature, so self-absorption could be neglected.

CALCULATIONS

The electronic oscillator strengths were determined by fitting the reduced experimental spectra to theoretical spectra which were calculated assuming the electronic oscillator strengths were unity. The calculation consists of several steps: first, calculating the

radiation per unit volume at every point in the shock layer; then integrating over those portions of the shock layer which can be seen by the spectrometer. If the radiating gas may be assumed to be both optically thin and everywhere in local thermodynamic equilibrium, the only unknowns are the oscillator strengths of the various radiating systems. The details of these steps are described below.

Radiation per Unit Volume

There are several method proposed for computing the radiation per unit volume from a hot gas.[7,8,9,10] The method chosen for use here was that of Williams and Treanor,[7] which has the advantage of being both straightforward and in a form which allows for extremely rapid calculation with a large digital computer. In addition, the assumptions and inherent precision of the Williams and Treanor method are compatible with the experiments reported herein.

Williams and Treanor assume that the shape of an electronic-vibrational band may be adequately represented by an averaged Q branch; that is, they choose $\Delta J = 0$, and take J, the rotational quantum number, as a continuous variable. This leads to a value of the absorption coefficient $k_{v'v''}$ of the form

$$k_{v'v''}(\nu) = C(v'v'') \exp\left[-\left(\frac{B'_v}{|B'_v - B''_v|}\right)\frac{hc(\nu-\nu^{o}_{v'v''})}{kT}\right] \qquad (1)$$

where $C(v'v'')$ is a quantity, independent of J, whose value is a function of the particular vibrational transition v'-v'', ν is the wave number, $\nu^{o}_{v'v''}$ is the band head wave number, and B''_v and B'_v are the rotational constants for the lower and upper electronic levels, respectively. The integral of the absorption coefficient over a single line

is written

$$\int k_{v'v''}\, d\nu = \frac{\pi e^2}{mc^2} N_l f_{v'v''} \tag{2}$$

where N_l is number of molecules in the absorbing state and $f_{v'v''}$ is the vibrational oscillator strength. Integrating Eq. (1) gives

$$\int k_{v'v''} d\nu = C'(v'v'')|B'_v - B''_v|(2J + 1) \exp[-B''_v J(J + 1)hc/kT] \tag{3}$$

N_l may be calculated since the density, temperature, and the partition functions for rotation, vibration, and electronic excitation are known, and thus $C(v'v'')$ may be evaluated if $f_{v'v''}$ is known, if Eq. (2) is equated with Eq. (3); $k_{v'v''}$ may then be calculated from Eq. (1). The absorption coefficient at any wave number is then equal to the $k_{v'v''}$ summed over all bands which contribute at that wave number. For a band system degraded to the violet,

$$k = \sum_{\nu_o \leq \nu} k_{v'v''} \tag{4}$$

and the radiation per unit volume from an optically thin gas is

$$I_\lambda = k'nB_\lambda \tag{5}$$

where n is the number density of radiating molecules, B_λ is the black-body intensity, and k' is the apparent absorption coefficient; that is, $k' = k[1 - \exp(-hc\nu/kT)]$. If more than one band system is present, the total radiation at any wavelength is the sum of I_λ for each system.

In the present work the rotational and vibrational constants were obtained from Herzberg (11) and the fraction of molecules in the various electronic states was taken from Gilmore (12). The procedure for obtaining $f_{v'v''}$ is discussed in detail below.

Radiation Observed

If the radiating gas is optically thin, the radiation at a given wavelength deduced from measurements like those in the present tests may be written

$$E_\lambda(\text{watts}/\mu) = \int_R^{R+\delta(\theta)} \int_0^{\theta} \int_0^{2\pi} I_\lambda(r,\theta,\varphi) F(\theta,\varphi) r^2 \sin\theta \, dr \, d\theta \, d\varphi \qquad (6)$$

Figure 5 shows the coordinate system; $F(\theta,\varphi)$ is the fraction of the volume not blocked from observation by the model. For a model flying with zero angle of attack the flow field is axisymmetric, so I_λ is not a function of the azimuth angle φ. Calculating I_λ as a function of r and θ requires a knowledge of the complete density and temperature field behind the bow shock. While methods for calculating inviscid density and temperature fields are becoming available for certain types of simple bodies,[13] these methods are, in general, long and expensive, and it was felt that such "exact" calculations would add little to the accuracy of the final results desired here. Instead the following approximate procedure was applied. The shock layer was assumed inviscid. The shock envelope was assumed spherical but not concentric with the body (cf. Fig. 6), and a correlation suggested by Seiff[14] was used to calculate the shock standoff distance. Shadowgraphs obtained during the tests proved the latter two assumptions quite adequate. A typical shadowgraph is shown in Fig. 6.

If the nitrogen shock tables of Ahtye and Peng[15] are combined with the tables of species distribution found in Treanor and Logan,[16] the temperature, density, species distribution and, hence, radiation per unit volume can be calculated for the gas immediately behind the bow

shock as a function of θ. Further, assuming isentropic flow for the dividing streamline and calculating the pressure distributions by the method of Kaattari[17] permits the radiation from the fluid adjacent to the body to be calculated as a function of θ. Then $I_\lambda(\theta)$ is taken as the mean of the values calculated at θ behind the shock and at the body. Since the variation of radiation per unit volume between the shock and the body at any given θ was never more than 20 percent, such a linear approximation would seem reasonable. The variation of I_λ with θ can be measured by the experimental technique described by Givens, et al.[18]

The above calculation procedure was followed at each band head until a complete spectrum was obtained over the range of wavelength covered by the experiment.

Oscillator Strengths

The vibrational or band oscillator strength $f_{v'v''}$ may be written in terms of the electronic oscillator strength[10] f

$$f_{v'v''} = f q_{v'v''}$$

or the electronic transition moment[19] R_e

$$f_{v'v''} = \frac{\nu}{3R_\infty} \left| \frac{R_e}{ea_o} \right|^2 q_{v'v''}$$

where $q_{v'v''}$ is the square of the overlap integral or Franck-Condon factor, R_∞ is the Rydberg constant for infinite mass, e is the charge of the electron, and a_o is the radius of the first Bohr orbit. Further, f and R_e may be functions of wavelength because of their dependence upon internuclear separation. This dependence is usually expressed by an experimentally determined variation of R_e with the r-centroid $(\bar{r})$

$$\bar{r} = \frac{\int \psi_{v'} \psi_{v''} r \, dr}{\int \psi_{v'} \psi_{v''} \, dr}$$

where $\psi_{v'}$ and $\psi_{v''}$ are the vibrational wave functions of the v' and v'' levels, respectively, and r is the internuclear separation.

In order to extract meaningful values of f or R_e, it is necessary to have accurate values of the Franck-Condon factors. Nicholls[20] has calculated Franck-Condon factors for the $N_2(2+)$ and $N_2^+(1-)$ systems, assuming a Morse potential. For the $N_2(2+)$ system the $q_{v',v''}$ seem satisfactory. On the other hand, for the $N_2^+(1-)$ system the $q_{v',v''}$ calculated using a Morse potential are suspect considering the anomalous shape of the potential curve of the B state of the N_2^+ molecule.*[21] For the present work f for the $N_2^+(1-)$ system was calculated using the experimental values of $f_{v',v''}$ reported by Nicholls,[22] normalized by his value of $f_{v',v''}$ at the 0-0 band and using Nicholls' Franck-Condon factor[20] only at the 0-0 band. This procedure retains Nicholls' experimentally determined variation of f with wavelength for $N_2^+(1-)$ without reliance on the less accurate values of $q_{v',v''}$.

RESULTS

The electronic oscillator strengths at the $\Delta v = 0$ bands of both systems were obtained by fitting the calculated spectra to the experimental spectra by matching the areas under the radiation per unit wavelength versus wavelength curves; that is,

*I am indebted to Miss M. Williams for bringing this to my attention.

$$f = \frac{\int_{\Delta v=0} W_\lambda \, d\lambda}{\int_{\Delta v=0} E_\lambda \, d\lambda}$$

where W_λ is the absolute experimental intensity. This procedure leads to an unambiguous evaluation of the f-numbers at $\Delta v = 0$ as the $\Delta v = 0$ bands of the two systems are not overlapping to any appreciable extent. Further, for the $N_2(2+)$ system, an experimental variation of f with wavelength was determined by similarly fitting the remaining bands. Figure 7 shows the comparison of the calculated spectra with the experimental spectra and it is seen that the agreement is quite good throughout the spectral range covered.

A basic assumption in the theoretical calculations used here is that the gas in the shock layer is in complete thermo-chemical equilibrium. It has been found in previous studies both in shock tubes[23] and ballistic ranges[3] that under certain circumstances the radiation observed may be considerably enhanced by radiation from the nonequilibrium relaxation zone behind the shock front. The possibility of an appreciable nonequilibrium contribution was investigated by varying the ambient density. In the reduction procedure used here, the nonequilibrium radiation would show up as an erroneously large f number, the value of which should approach the correct f number as the density is increased. Such variation of apparent f number with density was discovered and is shown in Fig. 8, where the apparent f number is plotted as a function of the calculated equilibrium density immediately behind the bow shock at $\theta = 0$. It is seen that the f number of both systems levels off to a constant value at densities greater than about 0.9 amagat, indicating that the assumption of equilibrium is valid only at the greater densities.

The f numbers at the $\Delta v = 0$ band determined in this manner are $f = 0.053 \pm 0.01$ for the $N_2^+(1-)$ system and $f = 0.057 \pm 0.01$ for the $N_2(2+)$ system. The limits of error are estimated from the uncertainties in calibration and in the various flow-field approximations.

Table I compares the f numbers in the present work with those reported in the literature. The Bennett and Dalby result has been scaled to the 0-0 band as in reference (22) so as to allow direct comparison with the present work. The results given here are seen to be in quite reasonable agreement with those of other workers despite considerable variations in experimental technique. This agreement is even better than it appears since the shock-tube results have been reported as upper limits[19] and any possible systematic error in the electron beam experiment due to cascading effects would cause the f number reported by Bennett and Dalby to be low.

The measured variation of the square of the transition moment with the r-centroid for $N_2(2+)$ is shown explicitly in Fig. 9. The agreement with the variation given by Nicholls[22] is good. The points of the other workers are taken directly from the article of Keck, et al.[19] and the r-centroids are from Wallace and Nicholls.[24]

CONCLUDING REMARKS

The technique of observing the radiating gas cap of a hypersonic projectile with a time-of-flight scanning spectrometer has been shown to yield quantitative molecular spectra consistent with previous results which were obtained with more conventional methods. The advantages of the method used here are very high signal-to-noise ratio, relatively

good resolution, and a continuously recorded spectrum.* The main disadvantage lies in the lack of complete knowledge of the source of radiation, that is, the hypersonic shock layer. As time goes on, undoubtedly our knowledge of the details of the flow field within the shock layer will improve and thus add to the precision of the method reported here.

ACKNOWLEDGMENTS

I should like to acknowledge the contributions of Messrs. William A. Page, Roger A. Craig, and William C. Davy, who participated in the initial design and calibration of the scanning spectrometer; Henry T. Woodward and John Paterson, who assisted in the programming; and Warren Norman, who operated the ballistic range. I should particularly like to thank Dr. C. E. Treanor for several valuable discussions and correspondence.

*Recently a technique has been presented using a scanning spectrometer with a shock tube which also yields a continuously recorded spectrum. (25)

REFERENCES

1. R. A. Allen, J. C. Camm, and J. C. Keck, J.Q.S.R.T., 1, pp. 269-77 (1961).

2. R. G. Bennett and F. W. Dalby, J. Chem. Phys., 31, pp. 434-41 (1959).

3. W. A. Page and J. O. Arnold, Shock-Layer Radiation of Blunt Bodies at Reentry Velocities, NASA TR R-193 (1964).

4. R. A. Craig and W. C. Davy, Thermal Radiation From Ablation Products Injected Into a Hypersonic Shock Layer, NASA TN D-1978 (1963).

5. C. St. Pierre, The Visible Emission From 1/2" Hypervelocity Models Measured with a Moving Target Scan Monochromator, CARDE TM AB-59 (1960).

6. R. Stair, R. G. Johnston, and E. W. Halbach, J. Res., Nat. Bur. Stand. 64A, no. 4, pp. 291-6 (1960).

7. M. J. Williams and C. E. Treanor, A Method for Calculating Diatomic Spectra Using a Digital Computer, Cornell Aero. Lab. Rep. QM-1626-A-5 (1962).

8. J. C. Keck, J. C. Camm, B. Kivel, and T. Wentink, Jr., Ann. Phys., 7, pp. 1-38 (1959).

9. R. G. Breene, Jr. and M. C. Nardone, J.Q.S.R.T., 2, p. 273 (1962).

10. R. W. Patch, W. L. Shackleford, and S. S. Penner, J.Q.S.R.T., 2, pp. 263-71 (1962).

11. G. Herzberg, Molecular Spectra and Molecular Structure. I. Spectra of Diatomic Molecules, 2nd ed., Van Nostrand Co., New York (1950).

12. F. R. Gilmore, Equilibrium Composition and the Thermodynamic Properties of Air to 24,000° K, Rand Corp. RM-1543 (1955).

13. F. B. Fuller, Numerical Solutions for Supersonic Flow of an Ideal Gas Around Blunt Two-Dimensional Bodies, NASA TN D-791 (1961).

14. A. Seiff, Recent Information on Hypersonic Flow Fields, Proceedings of the NASA University Conference, 2, p. 269 (1962).

15. W. F. Ahtye and T. Peng, Approximation for the Thermodynamic and Transport Properties of High-Temperature Nitrogen With Shock-Tube Applications, NASA TN D-1303 (1962).

16. C. E. Treanor and J. G. Logan, Jr., Thermodynamic Properties of Nitrogen from 2000° K to 8000° K, Cornell Aero. Lab. Rep. BE-1007-A-5 (1957).

17. G. E. Kaattari, Predicted Gas Properties in the Shock Layer Ahead of Capsule-Type Vehicles at Angles of Attack, NASA TN D-1423 (1962).

18. J. Givens, T. Canning, and H. Bailey, Measurements of Spatial Distribution of Shock-Layer Radiation for Blunt Bodies at Hypersonic Speeds, NASA TM X-852 (1964).

19. J. C. Keck, R. A. Allen, and R. L. Taylor, J.Q.S.R.T., 3, p. 335 (1963).

20. R. W. Nicholls, J. Res., Nat. Bur. Stand. 65A, pp. 451-60 (1961).

21. A. E. Douglas, Canad. J. Physics, 30, pp. 302-13 (1952).

22. R. W. Nicholls, J. Atmos. Terr. Phys., 25, pp. 218-21 (1963).

23. J. C. Camm, B. Kivel, R. L. Taylor, and J. D. Teare, J.Q.S.R.T., 1, pp. 53-75 (1961).

24. L. V. Wallace and R. W. Nicholls, J. Atmos. Terr. Phys., 7, pp. 101-5 (1955).

25. A. Fairbairn, AIAA preprint 63-454 (1963).

26. C. E. Treanor, Radiation at Hypersonic Speeds in "Hypersonic Flow Reasearch," F. R. Riddell, ed. Academic Press, New York, pp. 255-80 (1962).

TABLE I

Investigation	System	f	Excitation Technique
Bennett and Dalby	$N_2^+(1-)$	0.0438 ±0.002	Electron beam
	$N_2(2+)$	0.0425 ±0.005	
Allen, et al.	$N_2^+(1-)$	0.09 ±0.05*	Shock tube
Keck, et al.	$N_2(2+)$	0.007 ±0.05	Shock tube
Present work	$N_2^+(1-)$	0.053 ±0.01	Hypersonic projectile
	$N_2(2+)$	0.057 ±0.01	

*It has been observed[26] that a value of f = 0.06 would be a better fit to data presented in Ref. (1).

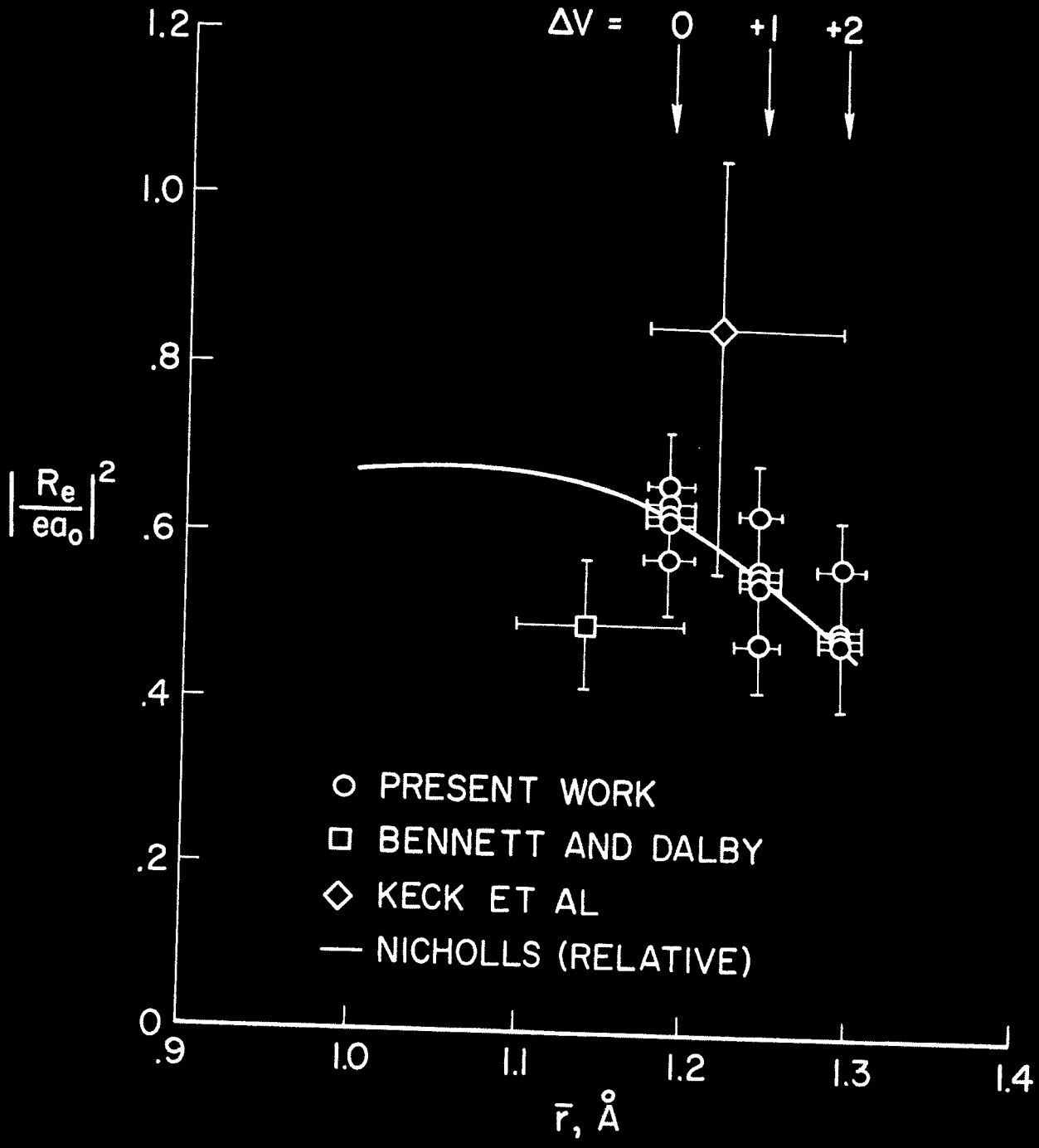

Fig. 9.- Transition probability as a function of r-centroid for $N_2(2+)$.

NATIONAL AERONAUTICS AND SPACE ADMINISTRATION
AMES RESEARCH CENTER, MOFFETT FIELD, CALIFORNIA

OSCILLATOR STRENGTHS FOR THE N_2 SECOND POSITIVE AND N_2^+ FIRST NEGATIVE SYSTEMS FROM OBSERVATIONS OF SHOCK LAYERS ABOUT HYPERSONIC PROJECTILES

By Victor H. Reis*

National Aeronautics and Space Administration
Ames Research Center
Moffett Field, Calif.

ABSTRACT

The electronic oscillator strengths, f, for the N_2 second positive and N_2^+ first negative systems were determined by measuring the radiation from the shock layer about a hypervelocity projectile with a time-of-flight scanning spectrometer. The measured values at the $\Delta v = 0$ bands were $f = 0.057 \pm 0.01$ for $N_2(2+)$ and $f = 0.053 \pm 0.01$ for $N_2(1-)$. The variation of f with wavelength for both systems was found to be similar to that previously reported by Nicholls.

INTRODUCTION

Measurements of radiant emission from shock-heated gases have been demonstrated[1] to yield values of oscillator strengths in reasonable agreement with values obtained by electron beam excitation.[2] In previous studies of radiation from shock-heated gases, the gas was energized by shock waves generated in shock tubes. The present investigation utilizes the gas in the shock layer behind the bow shock waves of small blunt models flying at hypersonic velocities into nitrogen as the source of radiation. Continuously recorded spectra are obtained photoelectrically by means of a time-of-flight scanning spectrometer

*Research Scientist

and reduced to obtain oscillator strengths (f-numbers) for the N_2 second positive $C^3\pi_u - B^3\pi_g$ and N_2^+ first negative $B^2\Sigma_u^+ - X^2\Sigma_g^+$ systems. Nitrogen was chosen as the test gas because of its relatively well-known thermodynamic and spectroscopic properties as well as its importance in atmospheric physics and as a contributor to the radiative heating of vehicles entering planetary atmospheres at hypersonic speeds.

EXPERIMENTAL TECHNIQUE

The models were lauched from the two-stage shock-heated 0.28-caliber light-gas gun of the pilot hypervelocity free-flight facility at the NASA, Ames Research Center.[3] The experimental setup is sketched in Fig. 1. The models were made of aluminum or a polyformaldehyde plastic. Because of the short flight distance the aerodynamic heating of the models was such that the aluminum surface remained relatively cool, whereas the surface of the plastic model ablated. However, as there was no measurable difference in the data obtained with the two different model materials, the plastic models were used more extensively since they were easier to launch successfully. In addition to the time-of-flight scanning spectrometer (described below) the instrumentation included shadowgraph stations and electronic counters to obtain the velocity and attitude of the model and an Abtronics 2HS image-converter camera. Relatively broad-band radiometers, each consisting of a multiplier phototube fitted with entrance and collimating slits and a band-pass filter, were used as a check on the over-all level of radiation seen by the scanning spectrometer. The radiometers also

allowed crude determination of the spatial distribution of radiation in the flow field. The use of such broad-band devices is described by Craig and Davy.(4)

Samples of the nitrogen were taken immediately prior to shooting and analyzed with a C.E.C. 21620 mass spectrometer. Typically, the contaminants, oxygen, argon, and water vapor, were held to trace amounts and never exceeded 0.2 percent.

TIME-OF-FLIGHT SCANNING SPECTROMETER

Spectra were obtained photoelectrically by means of a time-of-flight scanning spectrometer.* This device is shown schematically in Fig. 2. As the model flies by in the focal plane of the collecting mirror, the luminous gas cap acts as a moving entrance slit, sweeping out the spectrum of the shock-heated gas on the exit slit. (That the gas cap is the only source of radiation in the flow field and is indeed slitlike in form is shown in a typical image-converter photograph of a plastic model and in a typical oscillogram of a broad-band radiometer (Fig. 3).) The energy passing through the exit slit of scanning spectrometer is divided; 95 percent passes through a splitter plate and on to the cathode of an RCA 1P28 multiplier phototube. The output of this multiplier phototube is recorded on an oscilloscope and yields a continuously recorded spectrum over a wavelength range dictated mainly by the geometry of the system. For the tests reported in this work, the wavelength range was as a rule from 0.290 to 0.430 μ. Figure 4(a) shows a typical oscillogram. The remaining 5 percent of

*The concept for such a device appears to have originated with E. L. Woodcock and B. Jones.(5)

the energy passes through a narrow-band interference filter (100 Å half width) and onto a Dumont 6935 multiplier phototube. The output of this side band is displayed on an oscilloscope which has been triggered so as to start sweeping simultaneously with the oscilloscope which records the spectra. The side-band oscillogram thus allows a specific wavelength to be transposed to the oscillogram displaying the spectra. Such wavelength transposition was found to be repeatable from shot to shot to ±10Å.

The time-of-flight scanning spectrometer was constructed by modifying a Farrand uv-vis f/3.5 grating monochromator. A large opening was cut in the monochromator housing in the region of the entrance slit and the collecting mirror was replaced by a spherical mirror which focused at the center of the test chamber. Further, the new collecting mirror was masked down to a rectangular slot to improve depth of field and to insure uniform illumination of the grating. The rise time of the complete system was 25 nanoseconds and was dictated by the oscilloscope.

CALIBRATION

Wavelength calibration of the spectrometer was accomplished with a mercury lamp and appropriate color filters, both on a bench and in the test section. The complete optical train was calibrated with a tungsten ribbon filament lamp which had been previously compared with a primary standard supplied by the National Bureau of Standards.[6] The calibration curve for the complete optical train is shown in Fig. 4(b). The calibration was checked before and after each series of experiments.

EXPERIMENTAL RESULTS

Time-of-flight scanning spectrometer oscillograms were obtained for a range of model velocities of from 4.6 to 5.8 km/sec and ambient densities of 0.07 to 0.2 amagat. The calculated equilibrium temperatures throughout the shock layer ranged from 6000° to 7700° K. A typical oscillogram is shown in Fig. 4(a), and Fig. 4(c) shows this oscillogram reduced to absolute levels through the calibration curve (Fig. 4(b)). The wavelength scale on the oscillogram is nonlinear because the model flies on a tangent to the focal plane of the collecting mirror and because of slight nonlinearities in the oscilloscope horizontal sweep. Results such as shown in Fig. 4(c) were found to be quite reproducible. The wavelengths of the peaks were repeated to within ±10Å over the entire range of experiments or at about the limit of accuracy for reading the oscillogram. In addition two shots at almost identical flight conditions gave results which agreed within 10 percent in absolute levels of radiation.

The peak values of radiant intensity were never greater than 1 percent of an equivalent black body, calculated at an average shock-layer temperature, so self-absorption could be neglected.

CALCULATIONS

The electronic oscillator strengths were determined by fitting the reduced experimental spectra to theoretical spectra which were calculated assuming the electronic oscillator strengths were unity. The calculation consists of several steps: first, calculating the

radiation per unit volume at every point in the shock layer; then integrating over those portions of the shock layer which can be seen by the spectrometer. If the radiating gas may be assumed to be both optically thin and everywhere in local thermodynamic equilibrium, the only unknowns are the oscillator strengths of the various radiating systems. The details of these steps are described below.

Radiation per Unit Volume

There are several method proposed for computing the radiation per unit volume from a hot gas.[7,8,9,10] The method chosen for use here was that of Williams and Treanor,[7] which has the advantage of being both straightforward and in a form which allows for extremely rapid calculation with a large digital computer. In addition, the assumptions and inherent precision of the Williams and Treanor method are compatible with the experiments reported herein.

Williams and Treanor assume that the shape of an electronic-vibrational band may be adequately represented by an averaged Q branch; that is, they choose $\Delta J = 0$, and take J, the rotational quantum number, as a continuous variable. This leads to a value of the absorption coefficient $k_{v'v''}$ of the form

$$k_{v'v''}(\nu) = C(v'v'') \exp\left[-\left(\frac{B'_v}{|B'_v - B''_v|}\right)\frac{hc(\nu-\nu^{o}_{v'v''})}{kT}\right] \qquad (1)$$

where $C(v'v'')$ is a quantity, independent of J, whose value is a function of the particular vibrational transition v'-v'', ν is the wave number, $\nu^{o}_{v'v''}$ is the band head wave number, and B''_v and B'_v are the rotational constants for the lower and upper electronic levels, respectively. The integral of the absorption coefficient over a single line

is written

$$\int k_{v'v''}\, d\nu = \frac{\pi e^2}{mc^2} N_l f_{v'v''} \qquad (2)$$

where N_l is number of molecules in the absorbing state and $f_{v'v''}$ is the vibrational oscillator strength. Integrating Eq. (1) gives

$$\int k_{v'v''} d\nu = C'(v'v'')\,|B'_v - B''_v|(2J + 1)\, \exp[-B''_v J(J + 1)hc/kT] \qquad (3)$$

N_l may be calculated since the density, temperature, and the partition functions for rotation, vibration, and electronic excitation are known, and thus $C(v'v'')$ may be evaluated if $f_{v'v''}$ is known, if Eq. (2) is equated with Eq. (3); $k_{v'v''}$ may then be calculated from Eq. (1). The absorption coefficient at any wave number is then equal to the $k_{v'v''}$ summed over all bands which contribute at that wave number. For a band system degraded to the violet,

$$k = \sum_{\nu_o \leq \nu} k_{v'v''} \qquad (4)$$

and the radiation per unit volume from an optically thin gas is

$$I_\lambda = k'nB_\lambda \qquad (5)$$

where n is the number density of radiating molecules, B_λ is the black-body intensity, and k' is the apparent absorption coefficient; that is, $k' = k[1 - \exp(-hc\nu/kT)]$. If more than one band system is present, the total radiation at any wavelength is the sum of I_λ for each system.

In the present work the rotational and vibrational constants were obtained from Herzberg (11) and the fraction of molecules in the various electronic states was taken from Gilmore (12). The procedure for obtaining $f_{v'v''}$ is discussed in detail below.

Radiation Observed

If the radiating gas is optically thin, the radiation at a given wavelength deduced from measurements like those in the present tests may be written

$$E_\lambda(\text{watts}/\mu) = \int_R^{R+\delta(\theta)} \int_0^{\theta} \int_0^{2\pi} I_\lambda(r,\theta,\varphi) F(\theta,\varphi) r^2 \sin\theta \, dr \, d\theta \, d\varphi \qquad (6)$$

Figure 5 shows the coordinate system; $F(\theta,\varphi)$ is the fraction of the volume not blocked from observation by the model. For a model flying with zero angle of attack the flow field is axisymmetric, so I_λ is not a function of the azimuth angle φ. Calculating I_λ as a function of r and θ requires a knowledge of the complete density and temperature field behind the bow shock. While methods for calculating inviscid density and temperature fields are becoming available for certain types of simple bodies,[13] these methods are, in general, long and expensive, and it was felt that such "exact" calculations would add little to the accuracy of the final results desired here. Instead the following approximate procedure was applied. The shock layer was assumed inviscid. The shock envelope was assumed spherical but not concentric with the body (cf. Fig. 6), and a correlation suggested by Seiff[14] was used to calculate the shock standoff distance. Shadowgraphs obtained during the tests proved the latter two assumptions quite adequate. A typical shadowgraph is shown in Fig. 6.

If the nitrogen shock tables of Ahtye and Peng[15] are combined with the tables of species distribution found in Treanor and Logan,[16] the temperature, density, species distribution and, hence, radiation per unit volume can be calculated for the gas immediately behind the bow

shock as a function of θ. Further, assuming isentropic flow for the dividing streamline and calculating the pressure distributions by the method of Kaattari[17] permits the radiation from the fluid adjacent to the body to be calculated as a function of θ. Then $I_\lambda(\theta)$ is taken as the mean of the values calculated at θ behind the shock and at the body. Since the variation of radiation per unit volume between the shock and the body at any given θ was never more than 20 percent, such a linear approximation would seem reasonable. The variation of I_λ with θ can be measured by the experimental technique described by Givens, et al.[18]

The above calculation procedure was followed at each band head until a complete spectrum was obtained over the range of wavelength covered by the experiment.

Oscillator Strengths

The vibrational or band oscillator strength $f_{v'v''}$ may be written in terms of the electronic oscillator strength[10] f

$$f_{v'v''} = f q_{v'v''}$$

or the electronic transition moment[19] R_e

$$f_{v'v''} = \frac{\nu}{3R_\infty} \left| \frac{R_e}{ea_o} \right|^2 q_{v'v''}$$

where $q_{v'v''}$ is the square of the overlap integral or Franck-Condon factor, R_∞ is the Rydberg constant for infinite mass, e is the charge of the electron, and a_o is the radius of the first Bohr orbit. Further, f and R_e may be functions of wavelength because of their dependence upon internuclear separation. This dependence is usually expressed by an experimentally determined variation of R_e with the r-centroid $(\overline{r})$

$$\overline{r} = \frac{\int \psi_{v'} \psi_{v''} r \, dr}{\int \psi_{v'} \psi_{v''} \, dr}$$

where $\psi_{v'}$ and $\psi_{v''}$ are the vibrational wave functions of the v' and v'' levels, respectively, and r is the internuclear separation.

In order to extract meaningful values of f or R_e, it is necessary to have accurate values of the Franck-Condon factors. Nicholls[20] has calculated Franck-Condon factors for the $N_2(2+)$ and $N_2^+(1-)$ systems, assuming a Morse potential. For the $N_2(2+)$ system the $q_{v',v''}$ seem satisfactory. On the other hand, for the $N_2^+(1-)$ system the $q_{v',v''}$ calculated using a Morse potential are suspect considering the anomalous shape of the potential curve of the B state of the N_2^+ molecule.*[21] For the present work f for the $N_2^+(1-)$ system was calculated using the experimental values of $f_{v',v''}$ reported by Nicholls,[22] normalized by his value of $f_{v',v''}$ at the 0-0 band and using Nicholls' Franck-Condon factor[20] only at the 0-0 band. This procedure retains Nicholls' experimentally determined variation of f with wavelength for $N_2^+(1-)$ without reliance on the less accurate values of $q_{v',v''}$.

RESULTS

The electronic oscillator strengths at the $\Delta v = 0$ bands of both systems were obtained by fitting the calculated spectra to the experimental spectra by matching the areas under the radiation per unit wavelength versus wavelength curves; that is,

*I am indebted to Miss M. Williams for bringing this to my attention.

$$f = \frac{\int_{\Delta v=o} W_\lambda \, d\lambda}{\int_{\Delta v=o} E_\lambda \, d\lambda}$$

where W_λ is the absolute experimental intensity. This procedure leads to an unambiguous evaluation of the f-numbers at $\Delta v = 0$ as the $\Delta v = 0$ bands of the two systems are not overlapping to any appreciable extent. Further, for the $N_2(2+)$ system, an experimental variation of f with wavelength was determined by similarly fitting the remaining bands. Figure 7 shows the comparison of the calculated spectra with the experimental spectra and it is seen that the agreement is quite good throughout the spectral range covered.

A basic assumption in the theoretical calculations used here is that the gas in the shock layer is in complete thermo-chemical equilibrium. It has been found in previous studies both in shock tubes[23] and ballistic ranges[3] that under certain circumstances the radiation observed may be considerably enhanced by radiation from the nonequilibrium relaxation zone behind the shock front. The possibility of an appreciable nonequilibrium contribution was investigated by varying the ambient density. In the reduction procedure used here, the nonequilibrium radiation would show up as an erroneously large f number, the value of which should approach the correct f number as the density is increased. Such variation of apparent f number with density was discovered and is shown in Fig. 8, where the apparent f number is plotted as a function of the calculated equilibrium density immediately behind the bow shock at $\theta = 0$. It is seen that the f number of both systems levels off to a constant value at densities greater than about 0.9 amagat, indicating that the assumption of equilibrium is valid only at the greater densities.

The f numbers at the $\Delta v = 0$ band determined in this manner are $f = 0.053 \pm 0.01$ for the $N_2^+(1-)$ system and $f = 0.057 \pm 0.01$ for the $N_2(2+)$ system. The limits of error are estimated from the uncertainties in calibration and in the various flow-field approximations.

Table I compares the f numbers in the present work with those reported in the literature. The Bennett and Dalby result has been scaled to the 0-0 band as in reference (22) so as to allow direct comparison with the present work. The results given here are seen to be in quite reasonable agreement with those of other workers despite considerable variations in experimental technique. This agreement is even better than it appears since the shock-tube results have been reported as upper limits[19] and any possible systematic error in the electron beam experiment due to cascading effects would cause the f number reported by Bennett and Dalby to be low.

The measured variation of the square of the transition moment with the r-centroid for $N_2(2+)$ is shown explicitly in Fig. 9. The agreement with the variation given by Nicholls[22] is good. The points of the other workers are taken directly from the article of Keck, et al.[19] and the r-centroids are from Wallace and Nicholls.[24]

CONCLUDING REMARKS

The technique of observing the radiating gas cap of a hypersonic projectile with a time-of-flight scanning spectrometer has been shown to yield quantitative molecular spectra consistent with previous results which were obtained with more conventional methods. The advantages of the method used here are very high signal-to-noise ratio, relatively

good resolution, and a continuously recorded spectrum.* The main disadvantage lies in the lack of complete knowledge of the source of radiation, that is, the hypersonic shock layer. As time goes on, undoubtedly our knowledge of the details of the flow field within the shock layer will improve and thus add to the precision of the method reported here.

ACKNOWLEDGMENTS

I should like to acknowledge the contributions of Messrs. William A. Page, Roger A. Craig, and William C. Davy, who participated in the initial design and calibration of the scanning spectrometer; Henry T. Woodward and John Paterson, who assisted in the programming; and Warren Norman, who operated the ballistic range. I should particularly like to thank Dr. C. E. Treanor for several valuable discussions and correspondence.

*Recently a technique has been presented using a scanning spectrometer with a shock tube which also yields a continuously recorded spectrum.[25]

REFERENCES

1. R. A. Allen, J. C. Camm, and J. C. Keck, J.Q.S.R.T., 1, pp. 269-77 (1961).

2. R. G. Bennett and F. W. Dalby, J. Chem. Phys., 31, pp. 434-41 (1959).

3. W. A. Page and J. O. Arnold, Shock-Layer Radiation of Blunt Bodies at Reentry Velocities, NASA TR R-193 (1964).

4. R. A. Craig and W. C. Davy, Thermal Radiation From Ablation Products Injected Into a Hypersonic Shock Layer, NASA TN D-1978 (1963).

5. C. St. Pierre, The Visible Emission From 1/2" Hypervelocity Models Measured with a Moving Target Scan Monochromator, CARDE TM AB-59 (1960).

6. R. Stair, R. G. Johnston, and E. W. Halbach, J. Res., Nat. Bur. Stand. 64A, no. 4, pp. 291-6 (1960).

7. M. J. Williams and C. E. Treanor, A Method for Calculating Diatomic Spectra Using a Digital Computer, Cornell Aero. Lab. Rep. QM-1626-A-5 (1962).

8. J. C. Keck, J. C. Camm, B. Kivel, and T. Wentink, Jr., Ann. Phys., 7, pp. 1-38 (1959).

9. R. G. Breene, Jr. and M. C. Nardone, J.Q.S.R.T., 2, p. 273 (1962).

10. R. W. Patch, W. L. Shackleford, and S. S. Penner, J.Q.S.R.T., 2, pp. 263-71 (1962).

11. G. Herzberg, Molecular Spectra and Molecular Structure. I. Spectra of Diatomic Molecules, 2nd ed., Van Nostrand Co., New York (1950).

12. F. R. Gilmore, Equilibrium Composition and the Thermodynamic Properties of Air to 24,000° K, Rand Corp. RM-1543 (1955).

13. F. B. Fuller, Numerical Solutions for Supersonic Flow of an Ideal Gas Around Blunt Two-Dimensional Bodies, NASA TN D-791 (1961).

14. A. Seiff, Recent Information on Hypersonic Flow Fields, Proceedings of the NASA University Conference, 2, p. 269 (1962).

15. W. F. Ahtye and T. Peng, Approximation for the Thermodynamic and Transport Properties of High-Temperature Nitrogen With Shock-Tube Applications, NASA TN D-1303 (1962).

16. C. E. Treanor and J. G. Logan, Jr., Thermodynamic Properties of Nitrogen from 2000° K to 8000° K, Cornell Aero. Lab. Rep. BE-1007-A-5 (1957).

17. G. E. Kaattari, Predicted Gas Properties in the Shock Layer Ahead of Capsule-Type Vehicles at Angles of Attack, NASA TN D-1423 (1962).

18. J. Givens, T. Canning, and H. Bailey, Measurements of Spatial Distribution of Shock-Layer Radiation for Blunt Bodies at Hypersonic Speeds, NASA TM X-852 (1964).

19. J. C. Keck, R. A. Allen, and R. L. Taylor, J.Q.S.R.T., 3, p. 335 (1963).

20. R. W. Nicholls, J. Res., Nat. Bur. Stand. 65A, pp. 451-60 (1961).

21. A. E. Douglas, Canad. J. Physics, 30, pp. 302-13 (1952).

22. R. W. Nicholls, J. Atmos. Terr. Phys., 25, pp. 218-21 (1963).

23. J. C. Camm, B. Kivel, R. L. Taylor, and J. D. Teare, J.Q.S.R.T., 1, pp. 53-75 (1961).

24. L. V. Wallace and R. W. Nicholls, J. Atmos. Terr. Phys., 7, pp. 101-5 (1955).

25. A. Fairbairn, AIAA preprint 63-454 (1963).

26. C. E. Treanor, Radiation at Hypersonic Speeds in "Hypersonic Flow Reasearch," F. R. Riddell, ed. Academic Press, New York, pp. 255-80 (1962).

TABLE I

Investigation	System	f	Excitation Technique
Bennett and Dalby	$N_2^+(1-)$	0.0438 ±0.002	Electron beam
	$N_2(2+)$	0.0425 ±0.005	
Allen, et al.	$N_2^+(1-)$	0.09 ±0.05*	Shock tube
Keck, et al.	$N_2(2+)$	0.007 ±0.05	Shock tube
Present work	$N_2^+(1-)$	0.053 ±0.01	Hypersonic projectile
	$N_2(2+)$	0.057 ±0.01	

*It has been observed[26] that a value of $f = 0.06$ would be a better fit to data presented in Ref. (1).

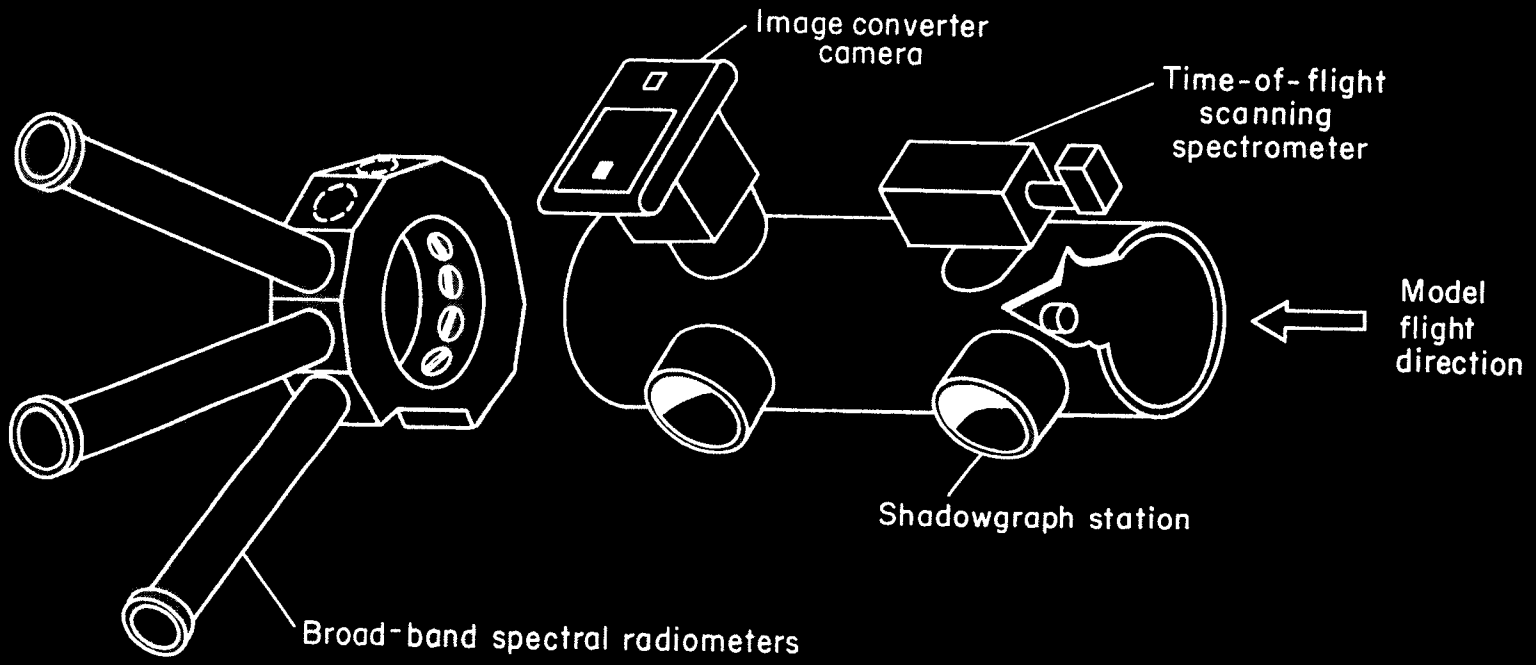

Fig. 1.- Sketch of test section.

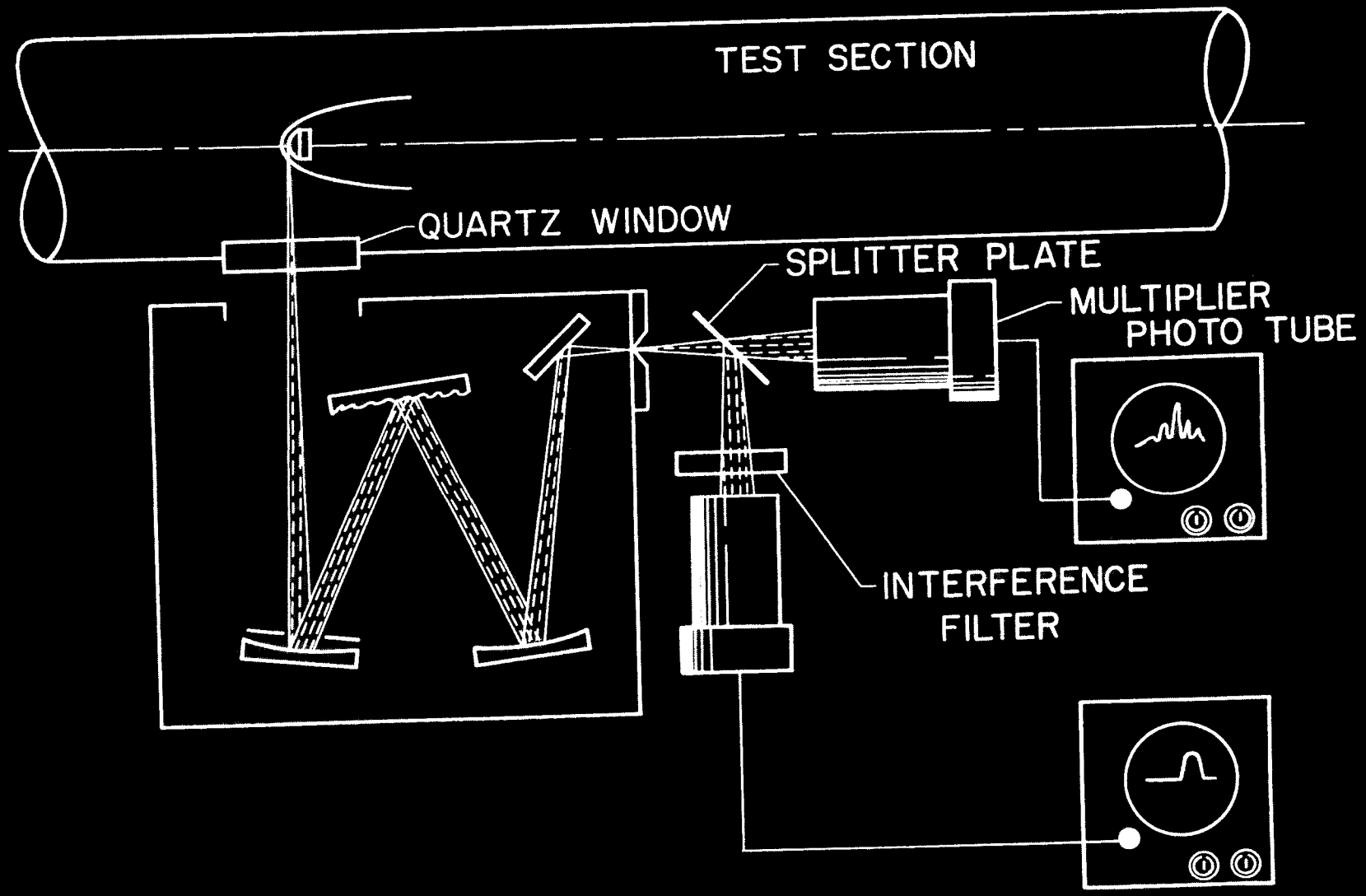

Fig. 2.- Time-of-flight scanning spectrometer.

NATIONAL AERONAUTICS AND SPACE ADMINISTRATION
AMES RESEARCH CENTER, MOFFETT FIELD, CALIFORNIA

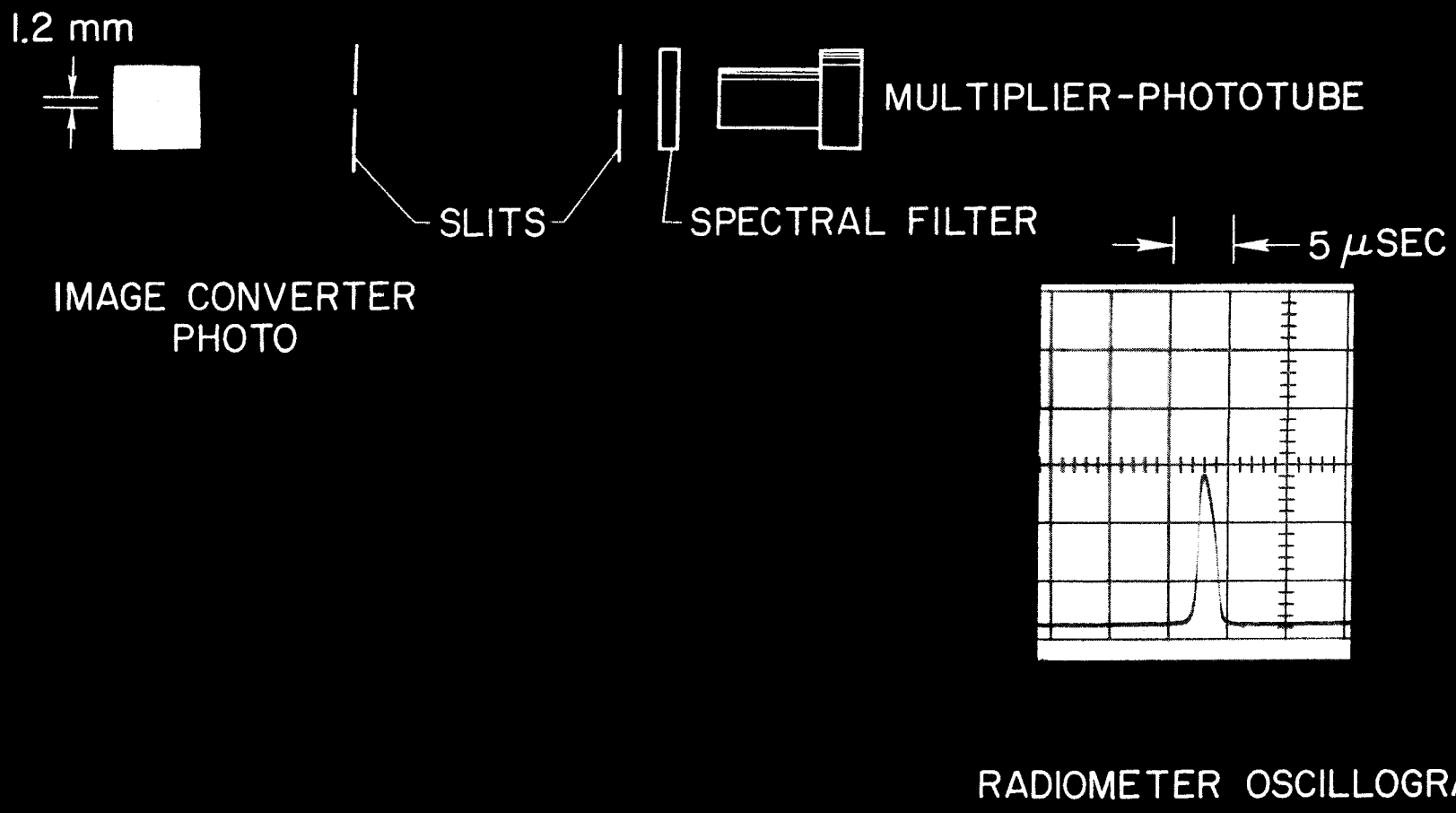

Fig. 3.- Image converter photograph and radiometer oscillogram showing slitlike appearance of shock layer.

NATIONAL AERONAUTICS AND SPACE ADMINISTRATION
AMES RESEARCH CENTER, MOFFETT FIELD, CALIFORNIA

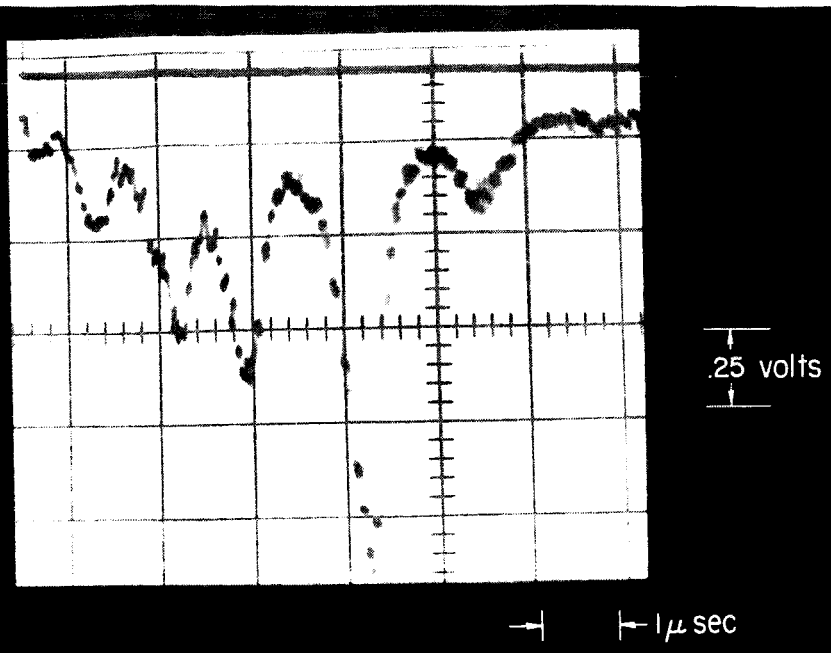

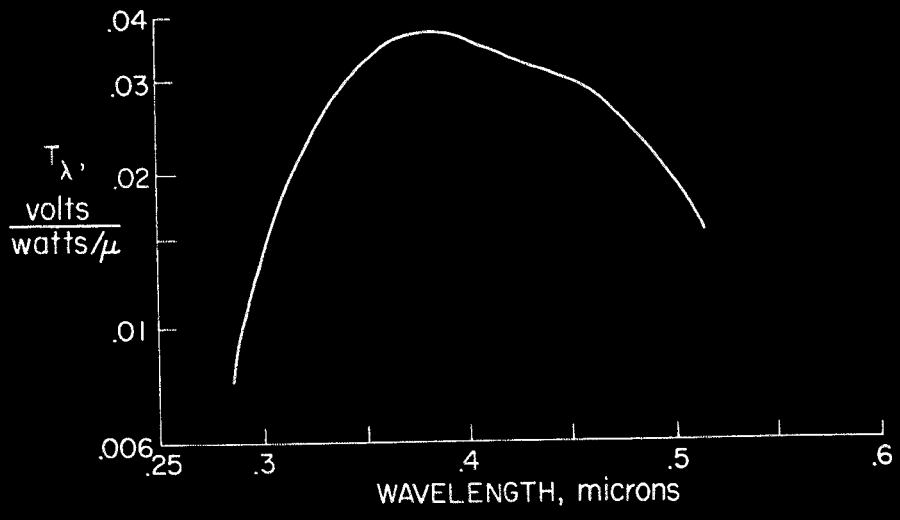

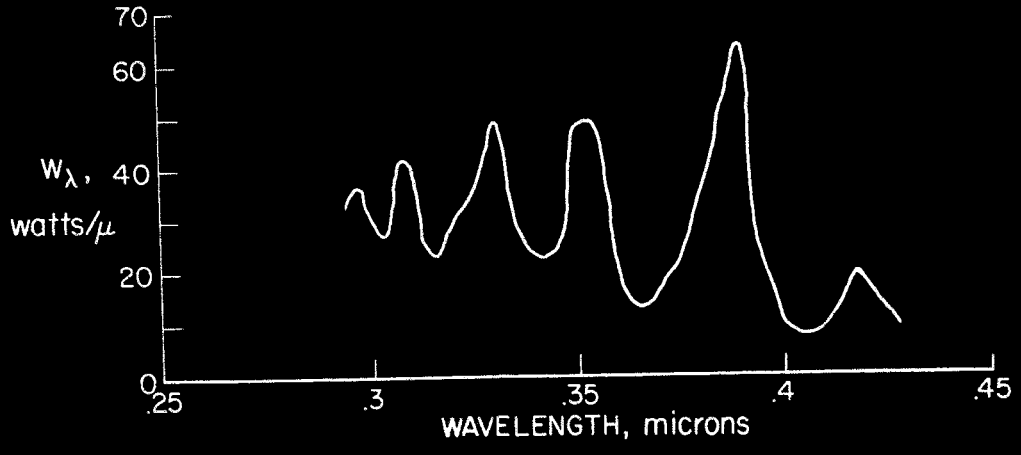

(a) Typical oscillogram from time-of-flight scanning spectrometer.
(b) Calibration curve of time-of-flight scanning spectrometer.
(c) Reduced experimental spectra.

Fig. 4.- Steps in determination of experimental spectra.

NATIONAL AERONAUTICS AND SPACE ADMINISTRATION
AMES RESEARCH CENTER, MOFFETT FIELD, CALIFORNIA

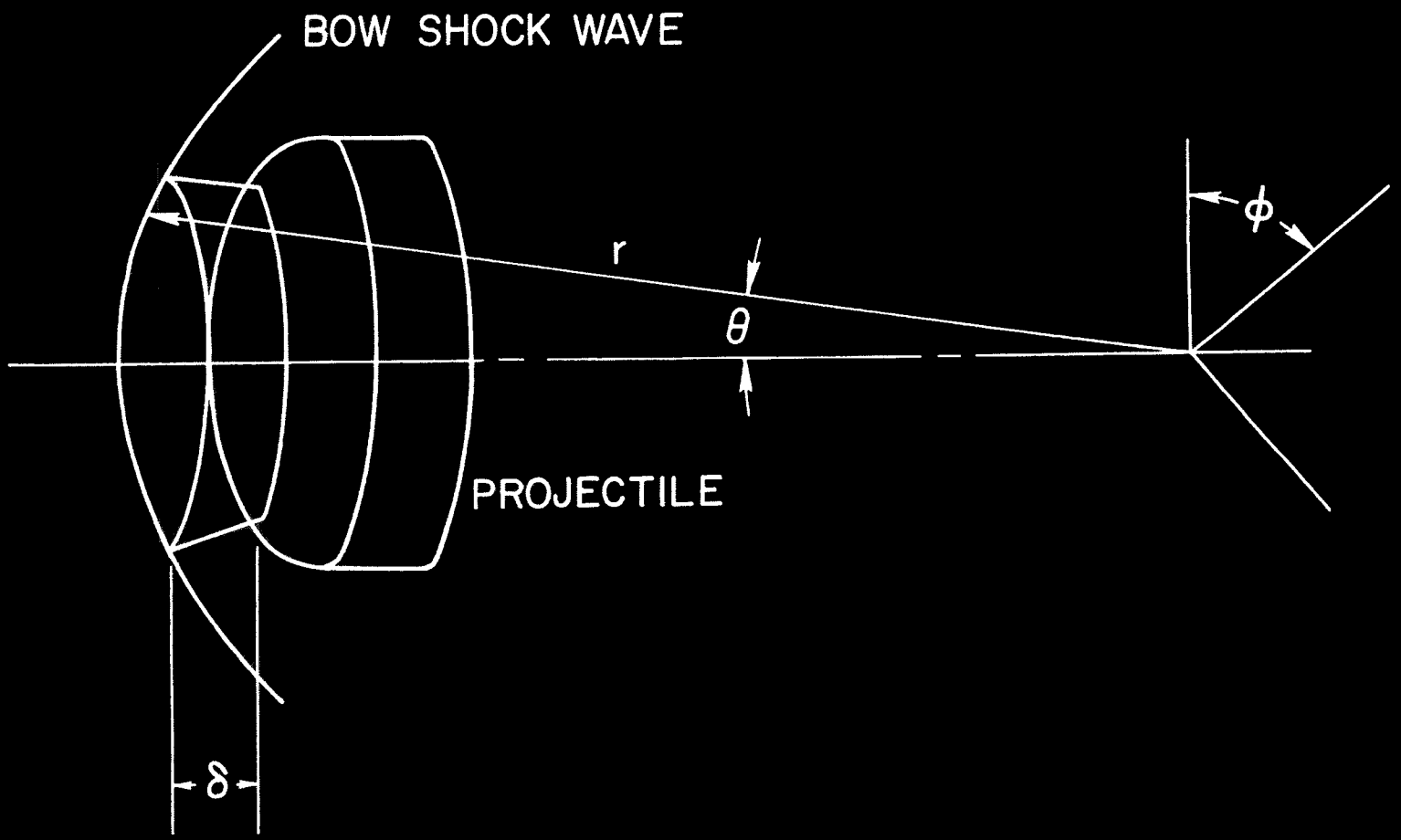

Fig. 5.- Coordinate system.

NATIONAL AERONAUTICS AND SPACE ADMINISTRATION
AMES RESEARCH CENTER, MOFFETT FIELD, CALIFORNIA

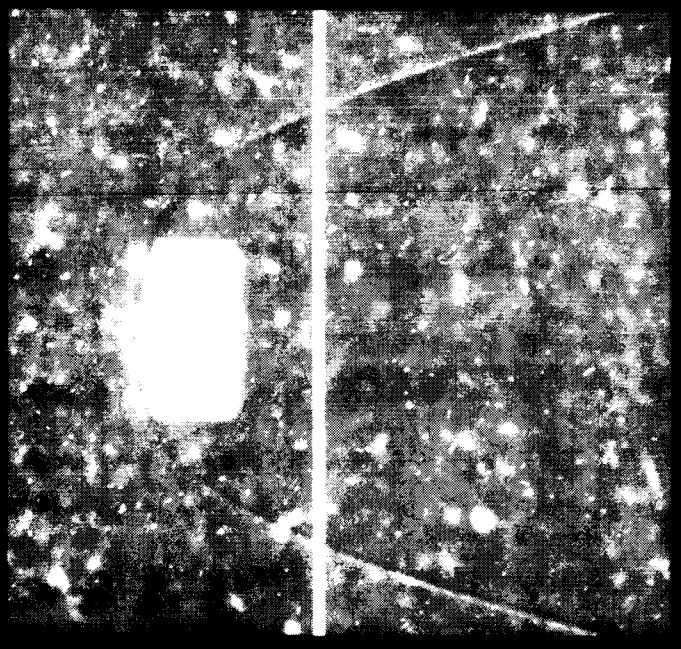

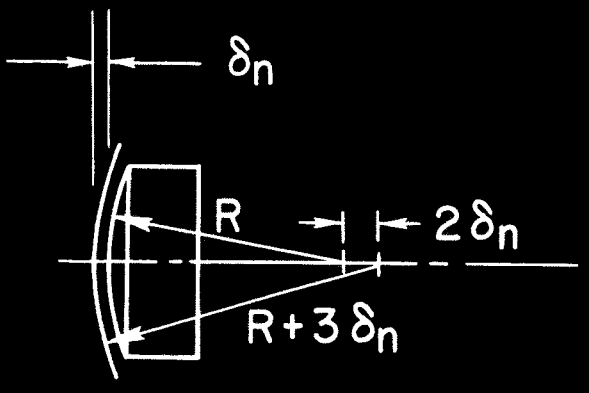

Fig. 6.- Typical shadowgraph of hypersonic projectile and assumed shock shape.

NATIONAL AERONAUTICS AND SPACE ADMINISTRATION
AMES RESEARCH CENTER, MOFFETT FIELD, CALIFORNIA

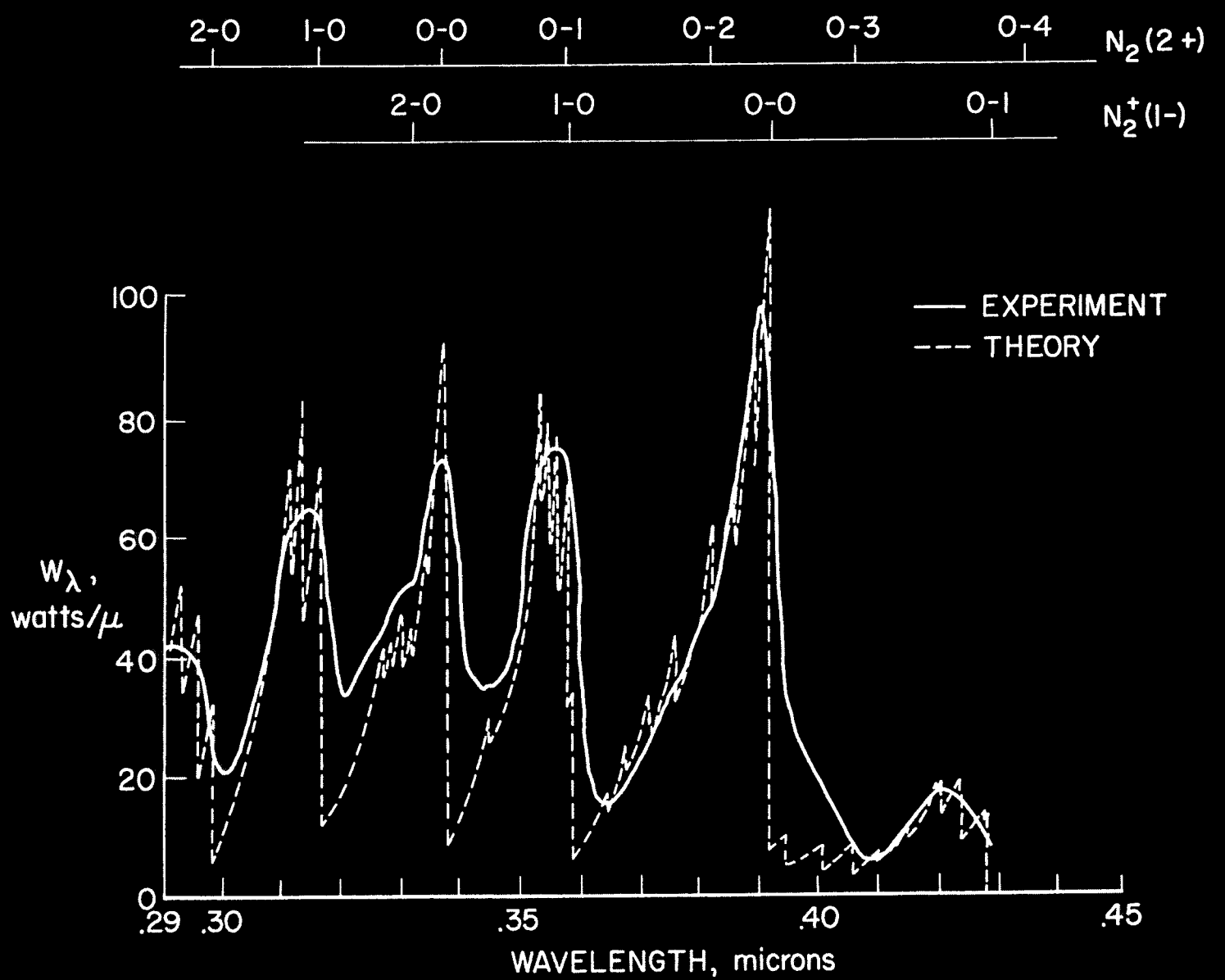

Fig. 7.- Comparison of calculated and experimental spectra.

NATIONAL AERONAUTICS AND SPACE ADMINISTRATION
AMES RESEARCH CENTER, MOFFETT FIELD, CALIFORNIA

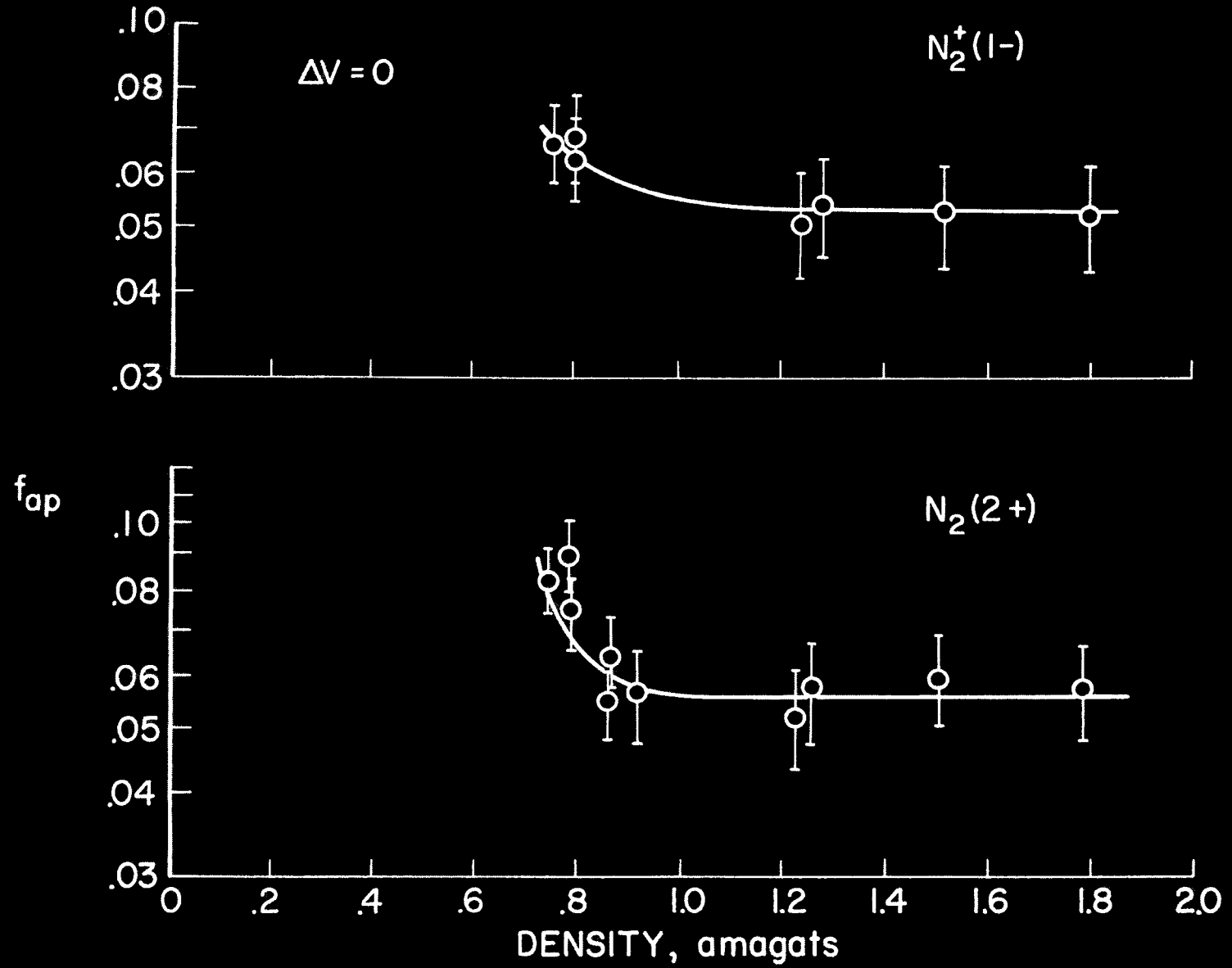

Fig. 8.- Variation of apparent f number with calculated equilibrium density behind bow shock.

NATIONAL AERONAUTICS AND SPACE ADMINISTRATION
AMES RESEARCH CENTER, MOFFETT FIELD, CALIFORNIA

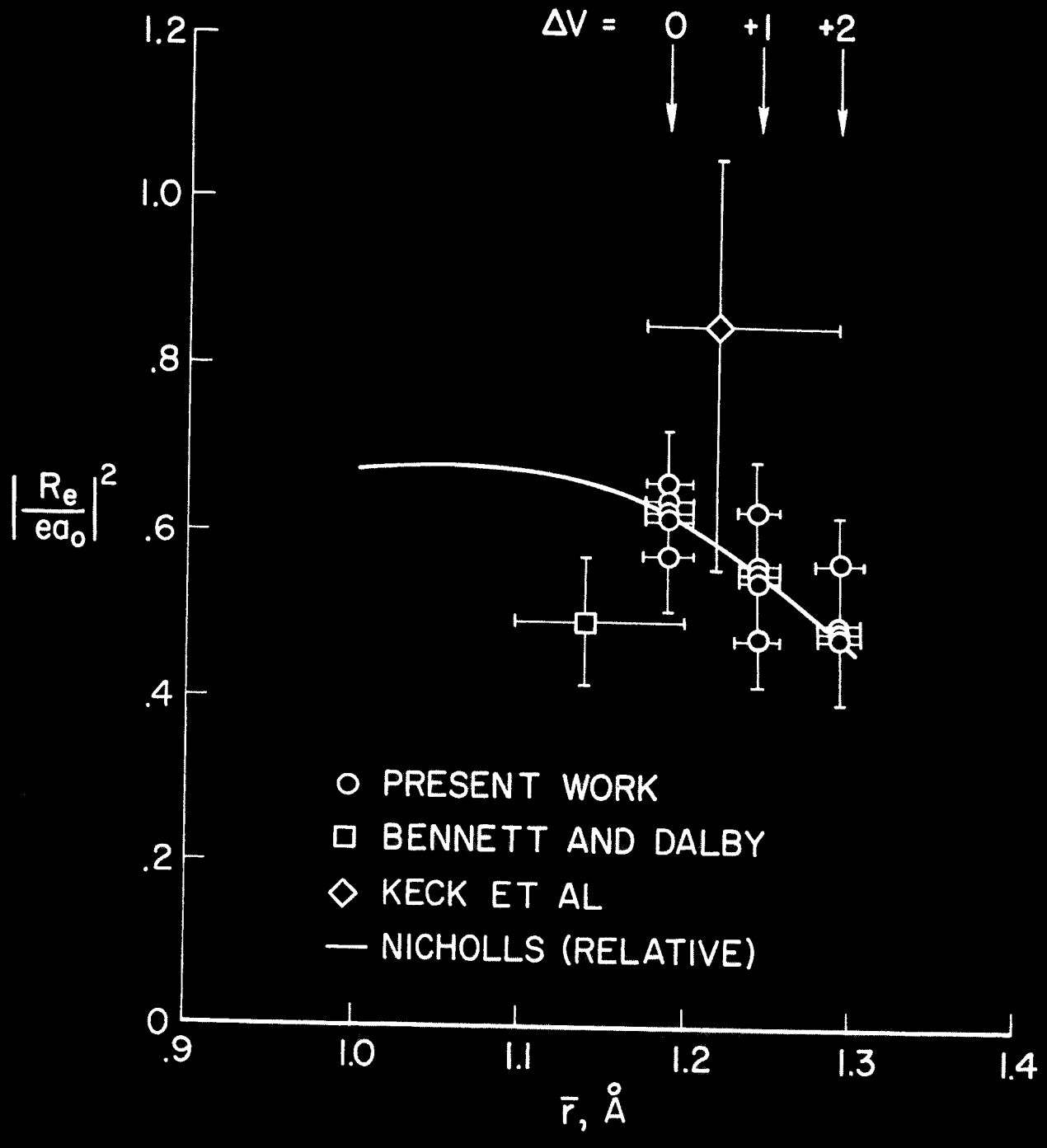

Fig. 9.- Transition probability as a function of r-centroid for $N_2(2+)$.

NATIONAL AERONAUTICS AND SPACE ADMINISTRATION
AMES RESEARCH CENTER, MOFFETT FIELD, CALIFORNIA